Summary

VNiVERSiDAD D SALAMANCA

CAMPUS OF INTERNATIONAL EXCELLENCE

DEPARTMENT OF CELL BIOLOGY AND PATHOLOGY

INSTITUTO DE NEUROCIENCIAS CASTILLA Y LEÓN

COMPARATIVE NEUROBIOLOGY LAB.

DOCTORAL THESIS

Nicotine-induced alterations during the development of the visual system of the zebrafish

Miguel Moyano Téllez

2013

INTRODUCTION

The zebrafish provides a good model for studying the development of the visual system of vertebrates. At early embryonic development, the primary visual field is located in the anterior neural plate (6 hpf). Once that the visual field has divided, optical primordia forms (10 $1/3$ hpf). Then these visual regions transformed into bistratified optical cups (retinal pigment epithelium and neural retina) (Schmitt and Dowling, 1994). Already in early stages of morphogenesis of the retina, the cells that compose the optical vesicles are morphologically and molecularly equivalent components that can generate the entire neural retina, the retinal pigmented epithelium and the optical peduncle. Simultaneously, the lens forms (at the stage of 21 somites, 19.5 hpf). At the stage of 48 hours post-fertilization, the eye is almost completely formed, but the choroidal fissure is not fully closed until hatching, approximately at 3 days post-fertilization. At 3 days post-fertilization all cell types and all layers of the retina are formed (Kimmel *et al.*, 2005).

The retina is a laminated structures that is formed by alternating layers of cells (inner nuclear layer, outer nuclear layer and ganglion cell layer) and neuropil (inner plexiform layer, outer plexiform layer and optic never fibre) with highly conserved cytoarchitecture in all vertebrates (Ramón y Cajal, 1892). The light crosses the vitreal face and, after passing through all retinal layers, incide on the photoreceptors, which transform the signal into electrical impulses that are transmitted to bipolar cells, and finally to ganglion cells (Dowling, 2012). The axons of these neurons form the optic nerve that exits the retina and project to the optic tectum that during the early stages of development have two layers: the white surface zone and the periventricular gray zone Vanegas *et al.*, 1984; Meek y Nieuwenhuys, 1998).

During the development of the visual system different molecular markers are expressed. This helps us analyze the different areas of the visual

pathway during ontogeny. We used in this study a marker for proliferation as phosphorylated histone H3, starting in the late G2 phase and extends around the nucleus during the M phase transition (Hendzel *et al.*, 1997). Also we used differentiation markers: Calretinin is abundantly expressed in the central and peripheral neural system, particularly in the retina, but also in other sensory pathways (Bertschy *et al.*, 1998). Zn-8 allows inmunolabeling ganglion cells and their growing axons (Westerfield, 1995). Islet-1 label ganglion cells when begin their differentiation (Sakagami *et al.*, 2003). Pax6a involved in the early development of the eye (MacDonald *et al.*, 1995, Wilson and MacDonald, 1996). and final distribution of specific cell populations as Tyrosine-hydroxylase for cells catecholaminergic, Zpr1 for cones and Zpr3 for rods.

The valuation of an innate response behavior should be as solid as possible, quantifiable and automated. Assays have been developed to conduct zebrafish larvae that have been used for mutation detection and characterization of the visual system of wild larvae vision and/or mutants. The tests used are optomotor was studied for Lyon (1904), optokinetic this test is a tool for detection of mutations that affecting the visual system of zebrafish larvae (Brockerhoff *et al.*, 1995, 1997; Neuhauss *et al.*, 1999, Gross *et al.*, 2005; Muto *et al.*, 2005). and visual-motor responses recordin the locomotor activity of the larvae in response to changes from light (McPhail *et al.*, 2009; Kokel *et al.*, 2010).

The electroretinogram (ERG) is a recording of the electrical activity of the whole retina. When a flash ERG is performed on a dark-adapted eye, the response derives primarily from the rod system. Sufficiently bright flashes will elicit ERGs containing mainly an a-wave (from photoreceptors) (Witkovsky *et al.,* 1975) and a b-wave (from bipolar, amacrine, and Müller cells) (Miller and Dowling, 1970; Newman and Odette,1984).

Tobacco addiction is one of the socio-economic and health major problems in developed countries and the prevalence of this disease is increasing

significantly in developing countries. According to the World Health Organization (WHO), more than one billion people smoke tobacco worldwide and its consumption produces more than 5 million deaths per year. Furthermore, tobacco consumption constitutes a risk factor for 6 of the 8 major causes of mortality worldwide (WHO, 2012). Nicotine is the main psychoactive component of tobacco and responsible for smoke addiction.

The effects of nicotine are a result of its action on the nicotinic acetylcholine receptor (nAChR) (Le Novere and Changeux, 1995), whose main function is the modulation of synaptic transmission. Recent findings indicate that acetylcholine can play an important role in nervous system development (Zoli *et al.*, 1995; Role and Berg, 1996). It has been determined from animal studies that the nicotinic acetylcholine receptor (nAChR) is functional from the early fetal development, when the neural tube is forming (Alturi *et al.*, 2001). Through the stimulation of nAChRs, acetylcholine can trigger neural development (Navarro *et al.*, 1989; Eriksson *et al.*, 2000). It has also been demonstrated that acetylcholine has a very active role in the development of the brain and is responsible for the proliferation, maturation and differentiation of many cell types (Kolb, 1989; Pugh and Margiota, 2000).

Studies of the effects of nicotine on neural development have demonstrated that failure occurs in early growth axonal (Svoboda *et al.*, 2002). It has also been shown that nicotine delayed differentiation of spinal motoneurons with involvement of nicotine-specific receptors (Higashijima *et al.*, 2000).

There is studies about alterations in the startle response in adult zebrafish exposed to nicotine during embryonic development (Eddins *et al.*, 2009). Persistent alterations in neuronal differentiation and axon growth have also been evaluated in adult zebrafish (Menelaou *et al.*, 2008), that had been previously described in embryos (Svoboda *et al.*, 2002). These findings on chronic effects in zebrafish complement those described it in rodents after prenatal

exposure to nicotine (Shacka *et al.*, 1997; Slotkin *et al.*, 2006). Exposure to nicotine during fetal development causes abnormalities in growth rates (Wang *et al.*, 2009) and alterations during nervous system development (Mao *et al.,* 2008).

Specific nicotinic receptors (α6 y β3) contribute to the organization and normal functioning of the visual system (Cui *et al.*, 2003; Gotti *et al.* 2005). The administration of nicotine can give rise to changes in the organization of this system, refining the visual topographic map (Yan *et al.*, 2006). Histopathological studies have shown that maternal intake of nicotine causes damage in newborn rat retina (Evereklioglu *et al.*, 2003). In animals treated with high doses of nicotine, the retinal ganglion cell layer and the overall thickness of the retina are reduced compared with control retinas. Selective degenerative changes were also observed in the inner plexiform layer, which is a characteristic shared with retinal ischemic atrophy (Evereklioglu *et al.*, 2003).

In this work, we have analyzed the morphogenesis of the zebrafish visual system in normal conditions and after exposure to nicotine in the 21-somite stage (19.5 hpf), when cellular differentiation events are initiated (Blader *et al.*, 2003; Quillien *et al.*, 2011). The analysis has been carried out under anatomical, neurochemical, electrophysiological and behavioral approaches.

OBJECTIVES

As hypothesis for this work we propose that nicotine affects the neurochemical expression pattern during development in different cell populations of the visual system, altering visual electrophysiological properties, which will result in changes on visually directed behavior. The specific objectives of the study are:

I.   Analysis of changes in the cytoarchitecture of the main components of the visual pathway after exposure to different concentrations of nicotine and at different stages of development.

II. Study of alterations in the neurochemical development of the visual pathway after exposure to nicotine, through the analysis of variations in expression patterns of different markers.

III. Analysis of changes in the expression of nAChRs that to specific to the visual pathway after exposure to nicotine at different stages of development.

IV. Study of the variations in the retinal electrophysiological response in animals exposed to nicotine.

V.   Analysis of the potential impact induced on the visual behavior after exposure to different concentrations of nicotine.

MATERIALS AND METHODS

The experiments were carried out in AB strain zebrafish embryos. They were staged and reared according to standard procedures (Westerfield, 1995). We have also used *nof* zebrafish mutants supplied by Prof. John E. Dowling, Harvard University (Cambridge, USA). *Nof* mutants exhibit a transition mutation in the gene for the α transducin (Tcα) of the cones, making it nonfunctional.

All procedures and experimental protocols were in accordance with the guidelines of the European Communities Directive (86/609/EEC, 2003/65/EC and 2010/63EU) and the current Spanish legislation for the use and care of animals in research (RD 1201/2005, BOE 252/34367-91, 2005).

Embryos were treated in the stage of 21 somites (19.5 hpf). Embryos were exposed to different concentrations of nicotine (5, 10, 20 y 40 µM) during different periods of time (until 48 hpf, 3 y 5 dpf). Untreated embryos were used as control specimens.

To assess the different objectives we used diverse experimental procedures including:

1. Morphometric measurements.

2. Quantification by HPLC.

3. Semithin sections stained with toloudine blue.

4. Whole-mount *in situ* hybridization using riboprobes (HIS).

5. *In toto* immunohistochemistry.

6. Immunohistochemistry in cryo-sections.

7. TUNEL technique.

8. Quantitative PCR.

9. Electroretinogram recording.

10. Behavioral analysis (optomotor, optokinetic and visual-motor responses).

11. Quantitative measurements were carried out by using ImageJ software, and Prism 4.0 (GrapPad) software was used for the statiscal analysis.

Riboprobes	Origin	Restriction enzymes	Polimerase
Islet-1	S. Wilson (Univeristy College London)	XbaI	T7
Pax6a	S. Wilson (Univeristy College London)	SmaI	T7
α6 nAChR	Own	HindIII	T7
ß3a nAChR	Own	HindIII	T7
ß3b nAChR	Own	XbaI	Sp6

Table 1: Riboprobes used in the study.

Antigen	Primary antibody	Dilution use	Source
Phosphorylated histone H3 (PH3)	Mouse monoclonal IgG	1:500	Abcam
Calretinin (CR)	Rabbit policlonal IgG	1:10000	Swant
Digoxigenin	Mouse monoclonal IgG	1:500	Jackson
Neuroline (Zn-8)	Mouse monoclonal IgG	1:250	Hibridoma bank
Tyrosine hydroxylase (TH)	Mouse monoclonal IgG	1:800	Chemicon
Zpr1	Rat monoclonal IgG	1:200	ZIRC
Zpr3	Rat monoclonal IgG	1:200	ZIRC

**Table 2**: Primary antibodies used in the study.

Summary

RESULTS

Morphological analysis

We have analyzed the changes in animal size and ocular parameters after nicotine treatment. In our study, we have not observed significant differences in the ocular size at 48 hpf, at any concentration of nicotine analyzed. At 3 dpf (Fig. 1) and 5 dpf, exposure to nicotine produces significant differences between treated animals and controls. The ventral and lateral ocular areas are significantly reduced. The treatment with nicotine reduces the ventral and lateral ocular projection area, the distance interocular and the eye and otolith. The reduction is higher in the groups of animals treated with nicotine concentrations of 20 and 40 µM.
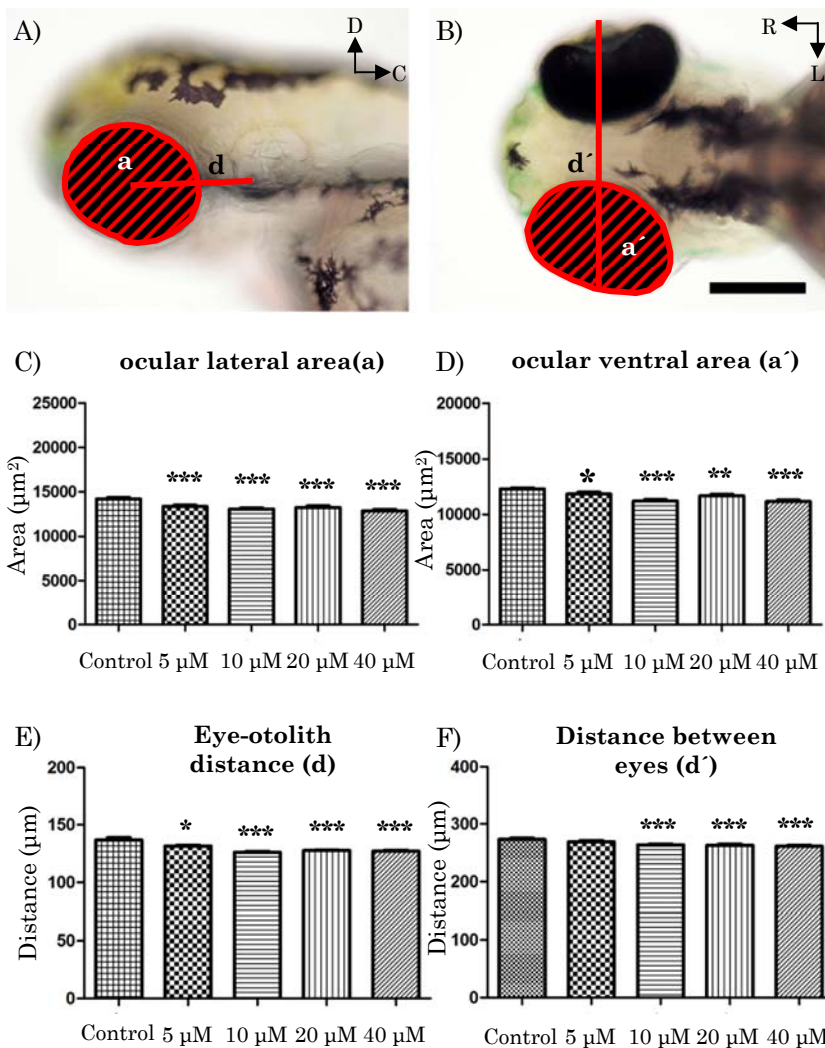
Fig. 1: A) Lateral view of a 3 dpf zebrafish embryo. a: projection area of left eye. d: distance between eyes and otolith. B) Ventral view from of a 3 dpf zebrafish embryo. a': projection area of left eye. d': distance between eyes. C), D), E) and F) Histograms of the ocular area and head morphometric distances of embryos in the different groups of study. C) Lateral ocular area. D) Ventral ocular area. E) Distance from the center of the eye to the otolith. F) Distance from the central end of one eye to the other eye. C: Caudal. D: Dorsal. L: Lateral. R: Rostral.
* = $P < 0.05$.
** = $0.05 > p > 0.001$.
*** = $P < 0.001$.
Scale bar: 100 µm.

We quantified the changes in the average size of the retina in the specimens treated with nicotine. In all cases, comparable anatomical regions were selected among all groups. At the stage of 48 hpf (Fig. 2) there is a small decrease in the retinal area in animals treated with nicotine compared to controls. The average size of the retinal area is $13,390 \pm 684.1$ µm². At the stages of 3 dpf (Fig. 2) the average size of the area of the retina ($16,490 \pm 616.2$ µm²) was significantly lower in the 40 µM treated animals with respect to the control group. At 5 dpf (Fig. 2) the decrease of the retinal area is larger than the previous stage, and the values are highly significant relative to those in control specimens, with an average area of the retina of $17,830 \pm 291.2$ µ m².
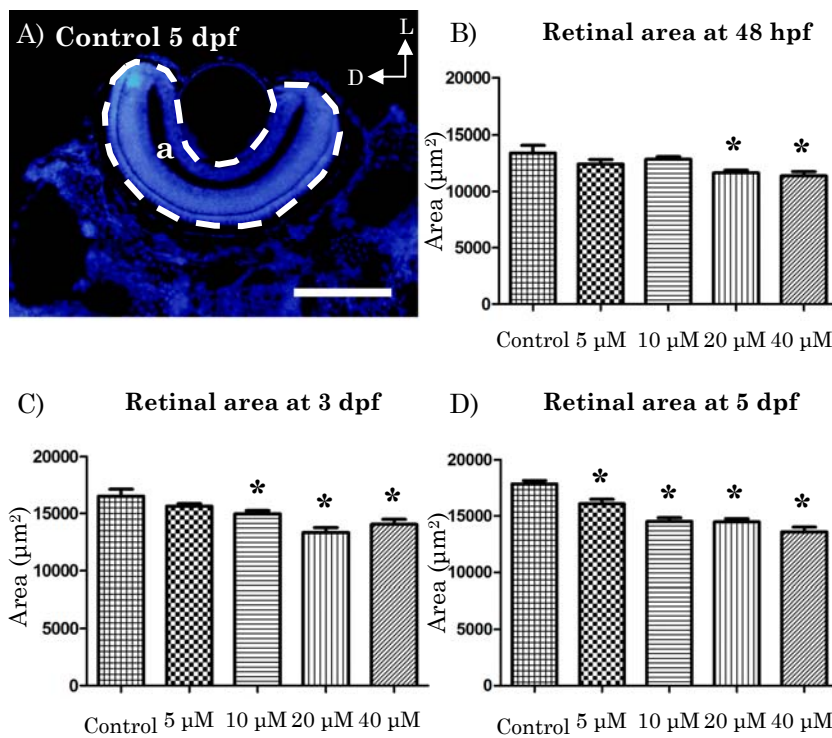
Fig. 2: A) Coronal section of an eye at 5 dpf. B), C) and D) Histograms of the area of the retina at different stages and treatments. B) Retinal area of 48 hpf embryos. C) Retinal area of 3 dpf larvae. D) Retinal area of 5 dpf larvae. a: area of a coronal section of a retina of 5 dpf. D: Dorsal. L: Lateral.
* = P <0.05.
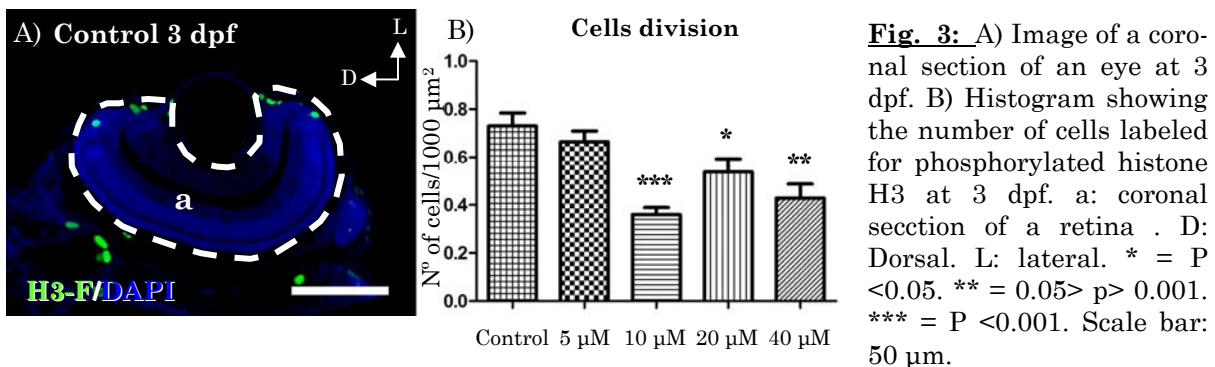** = 0.05> p> 0.001.
*** = P <0.001.
Scale bar: 50 µm.

Neurochemical analysis

We have analyzed the effect primary nicotine the on cell proliferation, cell differentiation and cell death in the visual areas of zebrafish. The study in an embryonic stage (48 hpf) and two larval stages (3 and 5 dpf).

We have analyzed the changes in cell proliferation by immunohistochemistry against phosphorylated histone H3. At the stage of 48

Summary

hpf, in animals treated with nicotine, the staining was observed in both lateral margins and in the central retinal area, with no significant differences with respect to the control group . At 3 dpf (Fig. 3) and 5 dpf, proliferating cells were observed in the ciliary margin, and in a lesser amount in the central area of the retina. The reduction in the number of proliferating cells with respect to controls maintains. The reduction is significant and the variations are associated to the concentrations of nicotine used.

Fig. 3: A) Image of a coronal section of an eye at 3 dpf. B) Histogram showing the number of cells labeled for phosphorylated histone H3 at 3 dpf. a: coronal secction of a retina . D: Dorsal. L: lateral. * = P <0.05. ** = 0.05> p> 0.001. *** = P <0.001. Scale bar: 50 µm.
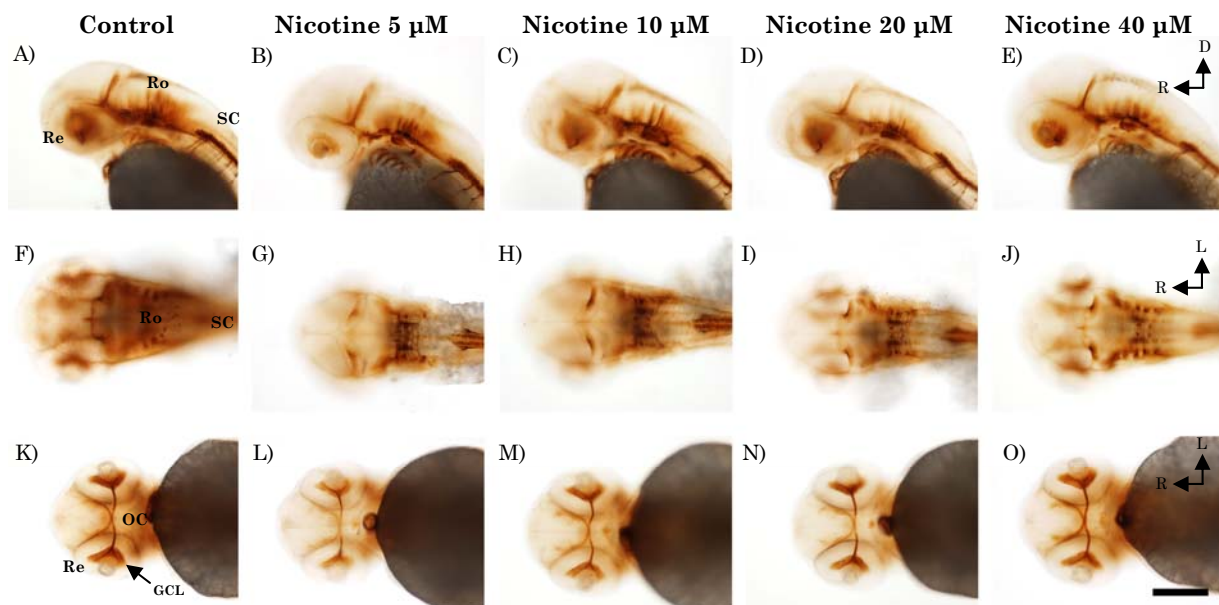
After TUNEL technique, apoptotic cells in the retina are a in both control and treated animals, with no significant differences between groups in any of the stages analyzed, or for the different concentrations tested.

The distribution of Calretinin positive elements in animals treated with nicotine was reduced after the nicotine treatment at 48 hpf and 3 dpf (Fig. 4), and it recovers with respect to the control group at the 5 dpf stage.

The number of immunoreactive elements for Zn-8 at 48 hpf (Fig. 5) decrease after nicotine treatment, in a inversely related manner to the concentration of nicotine administered. After hatching the number recovers, and is also maintained at the 5 dpf stage.
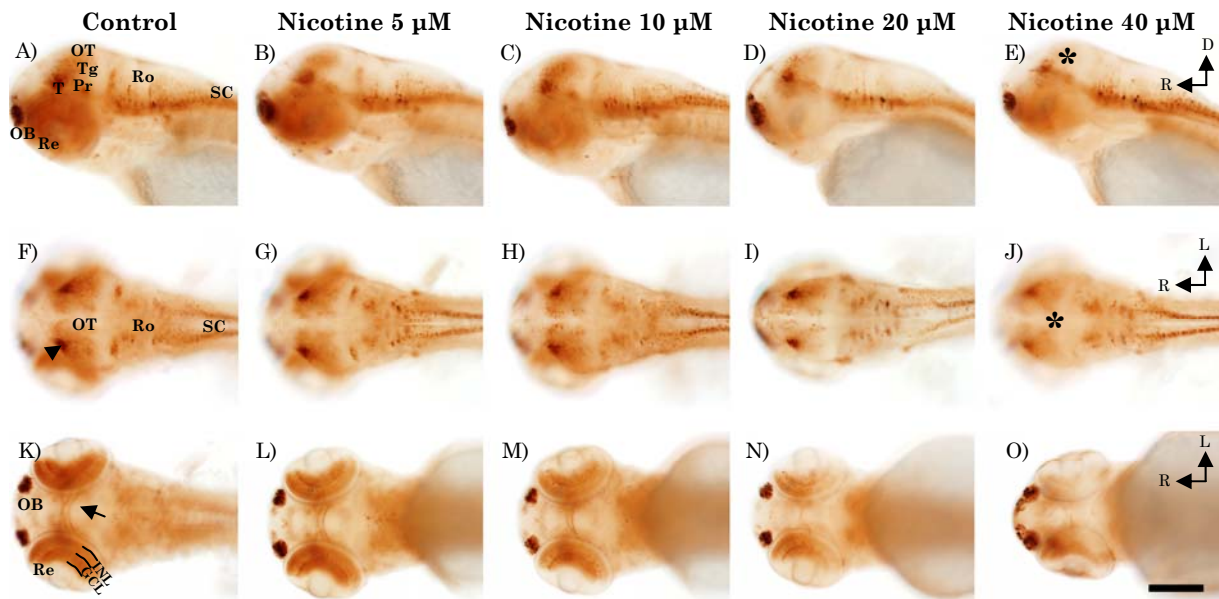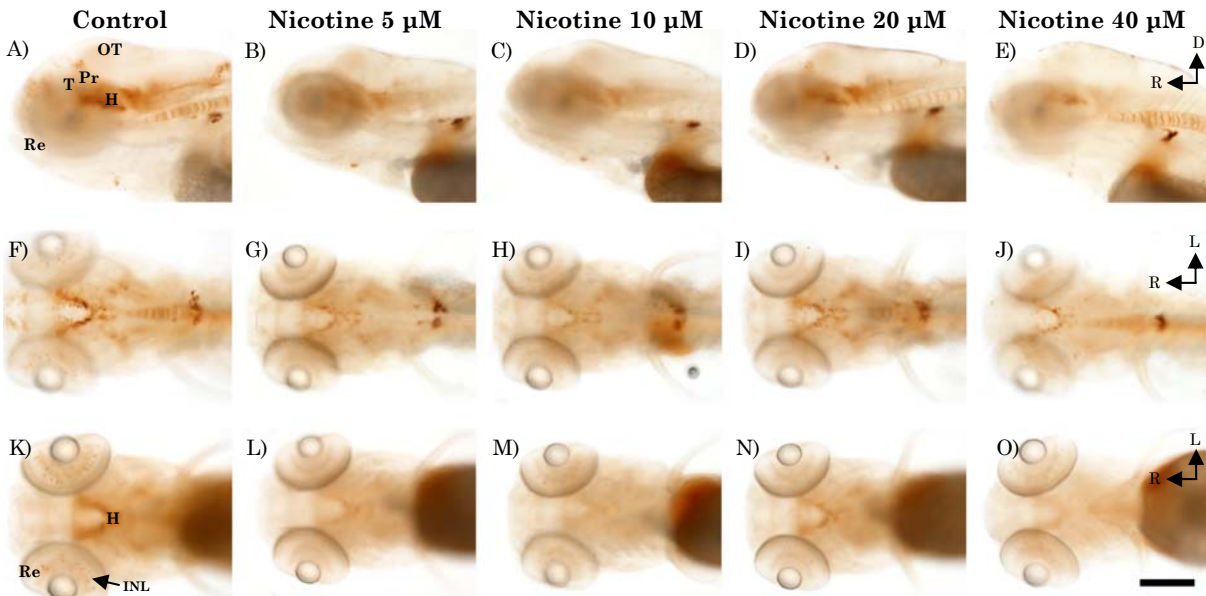
Fig. 4: *In toto* **immunohistochemistry for calretinin (CR) in 3 dpf larvae.** A)-E) Lateral view. F)-J) Dorsal view. K)-O) Ventral view. A), F) and K) Control animals, CR labeling is located in the olfactory bulbs, diencephalic structures as *pretectum,* and thalamus and in the rhombencephalon. At this stage there is also labeling in the OT (arrowhead), and in the retina in the GCL (arrow) and in the INL. In animals treated with nicotine the labeling for CR is reduced in the areas mentioned above. The nicotine 40 uM group shows a large decrease in OT labeling (asterisk), as occurs in the GCL of the retina. D: Dorsal. GCL: Ganglion cell layer. INL: Inner nuclear layer. L: Lateral. OB: Olfactory bulb. OT: Optic Tectum. Pr: *Pretectum*. R: Rostral. Ro: Rhombencephalon. T: Thalamus. Tg: *Tegmentum*. SC: Spinal cordal. Scale bar: 100 µm.

Fig. 5: *In toto* **immunohistochemistry for Zn-8 in 48-hpf embryos**. A)-E) Lateral view. F)-J) Dorsal view. K)-O) Ventral view. A), F) and K) Control embryo labeling for Zn-8 at the GCL of the retina (arrow) and optic nerves, which decussate in the optic chiasm and reach the TO. The animals treated with nicotine show a decreased staining for Zn-8 which is higher at lower concentration of nicotine administered. The concentration of 5 µM produces the highest marking reduction in optic nerves (asterisk). D: Dorsal. GCL: Ganglion cell layer. OC: Optic chiasm. R: Rostral. Re: Retina. Ro: Rhombencephalon. SC: Spinal cord. Scale bar: 100 µm.

The distribution pattern of Tyrosine-hydroxylase in animals treated with different concentrations of nicotine is less extensive labeling in visual areas, decreasing the projections that guide to different centers. These changes are more evident at higher doses and longer treatments (5 dpf) (Fig. 6).

Summary

Fig. 6: *In toto* **immunohistochemistry for TH in 5 dpf larvae.** A)-E) Lateral view. F)-J) Dorsal view. K)-O) Ventral view. A), F) and K) The control animals show staining in the hypothalamus, thalamus and *pretecum*. Note also the labeling in the OT (arrowhead). At this stage the rounded cells of the INL are marked (arrow). The nicotine-treated specimens show a remarkable reduction of staining for TH in the aforementioned regions. We did not observe any labeling for TH in nicotine treatment groups in the OT. D: Dorsal. H: Hypothalamus. INL: Inner nuclear layer. L: Lateral. OT: Optic tectum. Pr: *Pretectum*. R: Rostral. Re: Retina. T: Thalamus. Scale bar: 100 µm.

The expression of Islet-1 analyzed by HIS in nicotine treated animals show a reduction remarkable inversely to the concentration administered in all three stages of development analyzed (Fig. 7). The decrease was more evident at lower concentrations of nicotine.
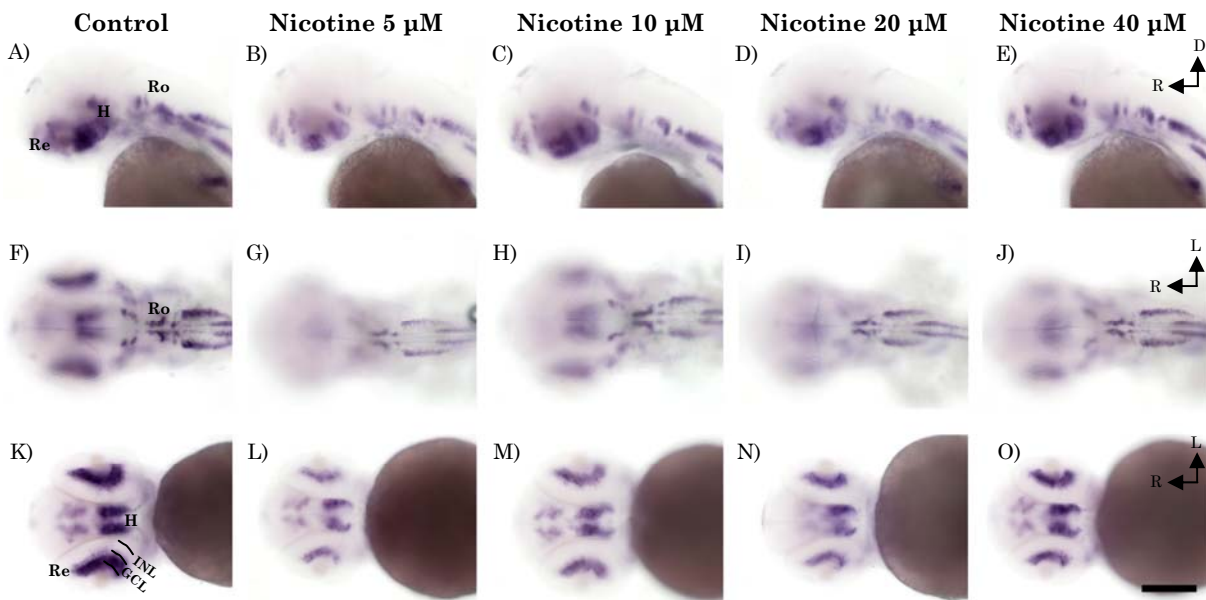
Fig. 7: *In toto in situ* **hybridization for Islet-1 in 48-hpf embryos.** A)-E) Lateral view. F)-J) Dorsal view. K)-O) Ventral view. A), F) and K) In the control group we observed labeling in the hypothalamus and in the GCL of the retina. The nicotine-treated specimens show a marked decrease of Islet-1 expression in visual structures that were also labeled in the control group. The modification was greater at lower concentrations of nicotine administered. Animals being treated with 5 µM present the higher alteration. D: Dorsal. GCL: Ganglion cell layer. H: Hypothalamus. INL: inner nuclear layer. L: Lateral. R: Rostral. Re: Retina. Ro: Rhombencephalon. Scale bar: 100 µm.

After Pax6a immunohistochemistry in animals treated with different concentrations of nicotine the expression pattern shows a decrease which is maintained at the three stages of development analyzed (Fig. 8). This reduction is higher for the highest concentration of nicotine used.

| | Control | Nicotine 5 µM | Nicotine 10 µM | Nicotine 20 µM | Nicotine 40 µM |
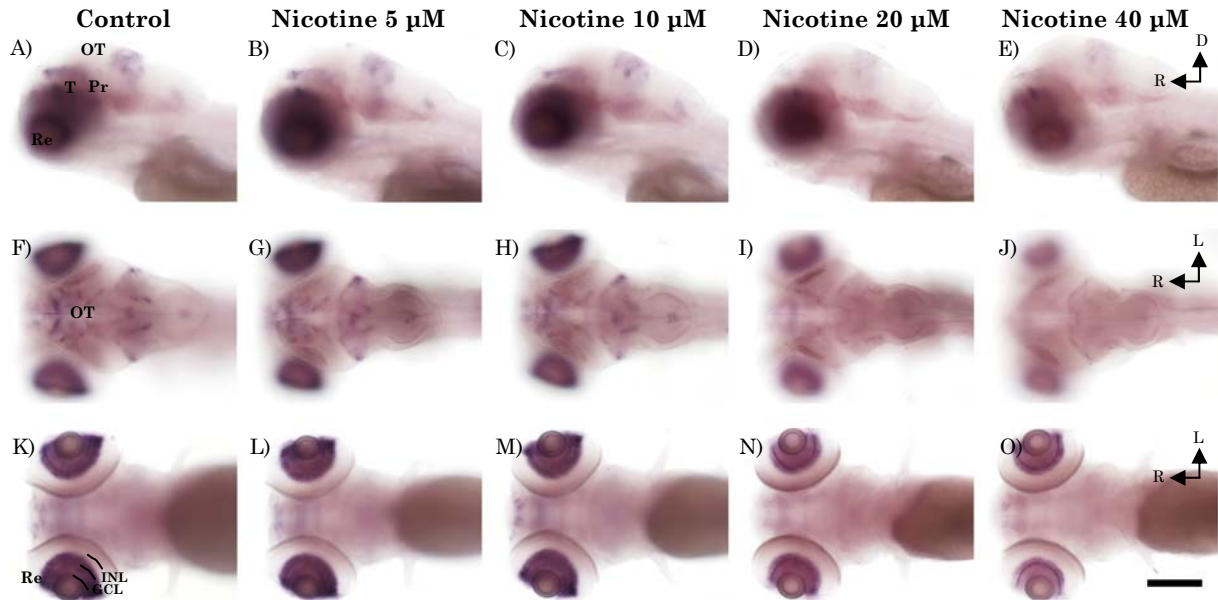
Fig. 8: *In toto in situ* **hybridization for Pax6a in 5 dpf larvae.** A)-E) Lateral view. F)-J) Dorsal view. K)-O) Ventral view. A), F) and K) Control group shows labeling in the thalamus and *pretectum*. At this stage of development there is expression in the OT in its rostralmost region. No expression was observed in the GCL and INL of the retina . The nicotine treated animals show a reduction in the expression of Pax6a in the visual structures mentioned in the control group. D: Dorsal. GCL: Ganglion cell layer. INL: Inner nuclear layer. L: Lateral. Pr: *Pretectum*. R: Rostral. Re: Retina. T: Thalamus. OT: Optic tectum. Scale bar: 100 µm.

We observed labeling for Zpr1, a marker specific for cone photoreceptors, in both larval stages analyzed, and there are no significant differences in the number of cones in the retina after the nicotine treatment with respect to the control groups.

We have analyzed at 3 dpf and 5 dpf the density of Zpr3, a marker specific for rod photoreceptors in animals treated with different concentrations of nicotine (Fig. 9) and we found a significant increase in the average number of rods per retina in both larval stages, more pronounced at 3 dpf.
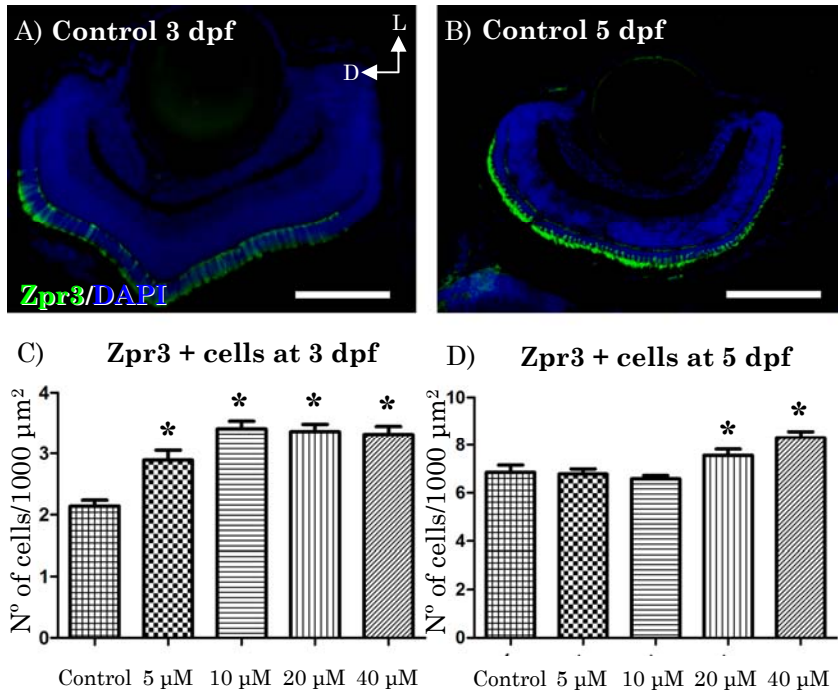
Fig. 9: A) Image of a coronal section of an eye at 3 dpf. B) Image of a coronal section of an eye at 5 dpf C) and D) Histograms for Zpr1 labeled cells in the retina. C) 3 dpf larvae. D) 5 dpf larvae. In animals treated with nicotine, we observed at the stage of 3 dpf that there is a significant increase in the number of rods in all concentrations of nicotine administred. At 5 dpf the significant increase in rods is only maintained at the higher dose of nicotine. D: Dorsal. L: lateral. * = P <0.05. Scale bar: A) 50 µm. B) 100 µm.

Analysis of the expresión of nAChRs in the visual pathway

We quantified the expression of the α6, ß3a and ß3b nAChR subunits that are present in the zebrafish visual pathway. We analyzed by quantitative PCR and HIS the pattern of expression of these receptors, comparing the results after treatment with different concentrations of nicotine with those from control animales.

The qPCR experiments showed an increase in α6 nAChR expression (Fig. 10A) over time of exposure to nicotine, which is more significant at higher concentrations. At low nicotine concentrations, the expression of this receptor increases slightly at the different stages analyzed. The values are very close to 1, similarly to the values obtained in the control group. In animals exposed to higher concentrations of nicotine, no differences in the expression with the control group were observed at 48 hpf. At 3 dpf and 5 dpf we observed a significant increase in the expression of this receptors with respect the control group.
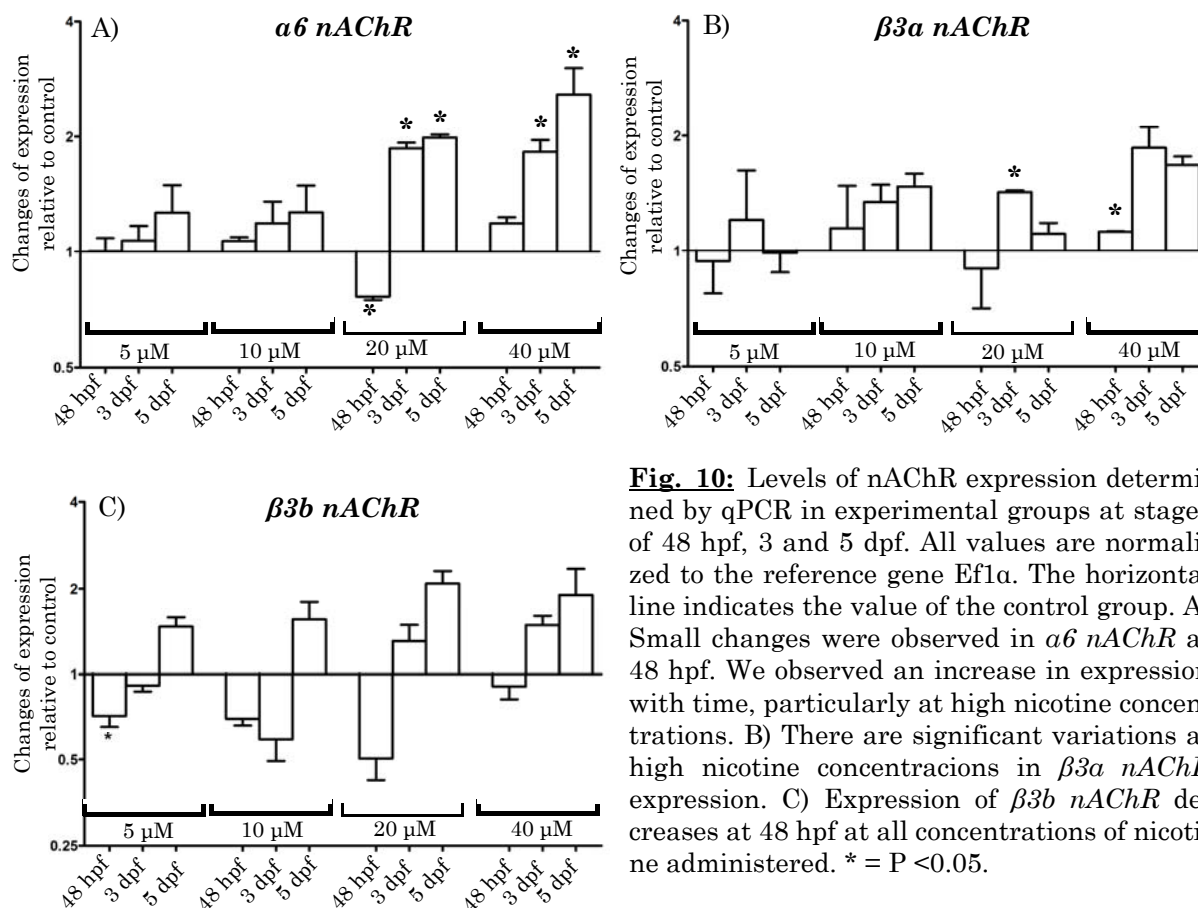
Fig. 10: Levels of nAChR expression determined by qPCR in experimental groups at stages of 48 hpf, 3 and 5 dpf. All values are normalized to the reference gene Ef1α. The horizontal line indicates the value of the control group. A) Small changes were observed in *α6 nAChR* at 48 hpf. We observed an increase in expression with time, particularly at high nicotine concentrations. B) There are significant variations at high nicotine concentracions in *ß3a nAChR* expression. C) Expression of *ß3b nAChR* decreases at 48 hpf at all concentrations of nicotine administered. * = P <0.05.

After HIS. the labeling for the α6 subunit of the nAChR is localized the GCL of the retina. This receptor subunit is also expressed in the OT and in nonvisual structures, as the pineal gland and the trigeminal ganglion. At the larval stages of 3 dpf (Fig.11) and 5 dpf, the labeling was observed in the GCL and in the INL of the retina, and in the OT.

After quantifying the expression of ß3a nAChR (Fig. 10B) we observed that the differences were dependent on the concentration of nicotine administered. In animals treated with 5 µM, no major changes in expression were observed at the different stages analyzed, with values close to 1. The specimens treated with 10 µM show slight increase of the expression over time of exposure, but without significant differences. At 3 dpf, with a concentration of 20 µM of nicotine, there is a significant increase in ß3a nAChR expression; this expression decreases at 5 dpf. In the specimens treated with the highest concentration (40 µM), a significant increase is detected over time.
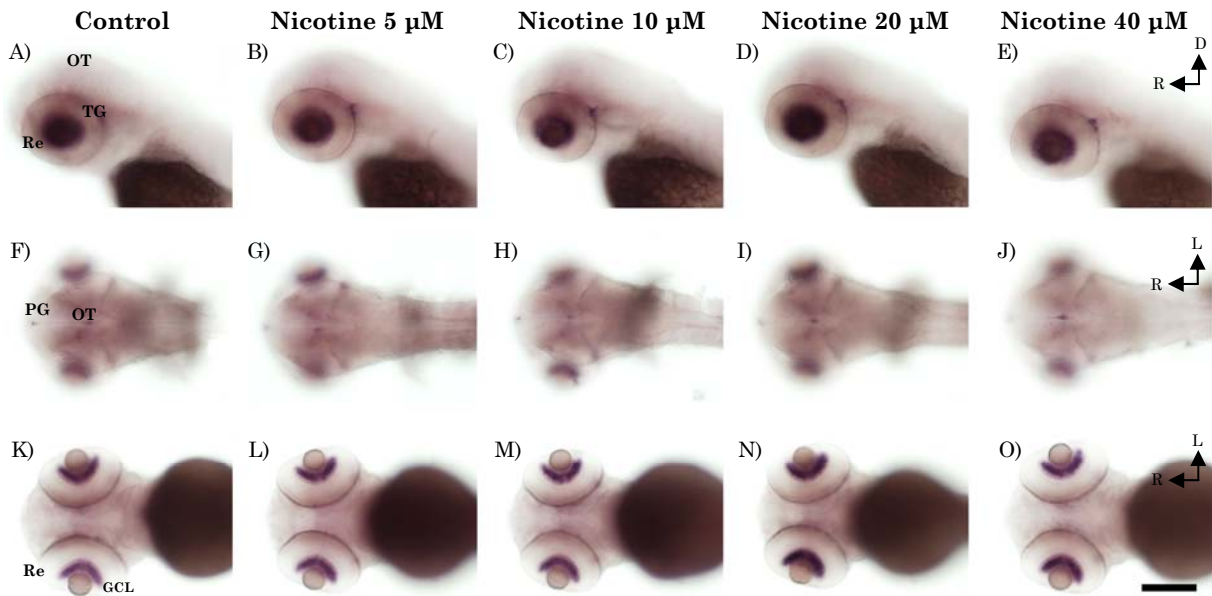
Summary
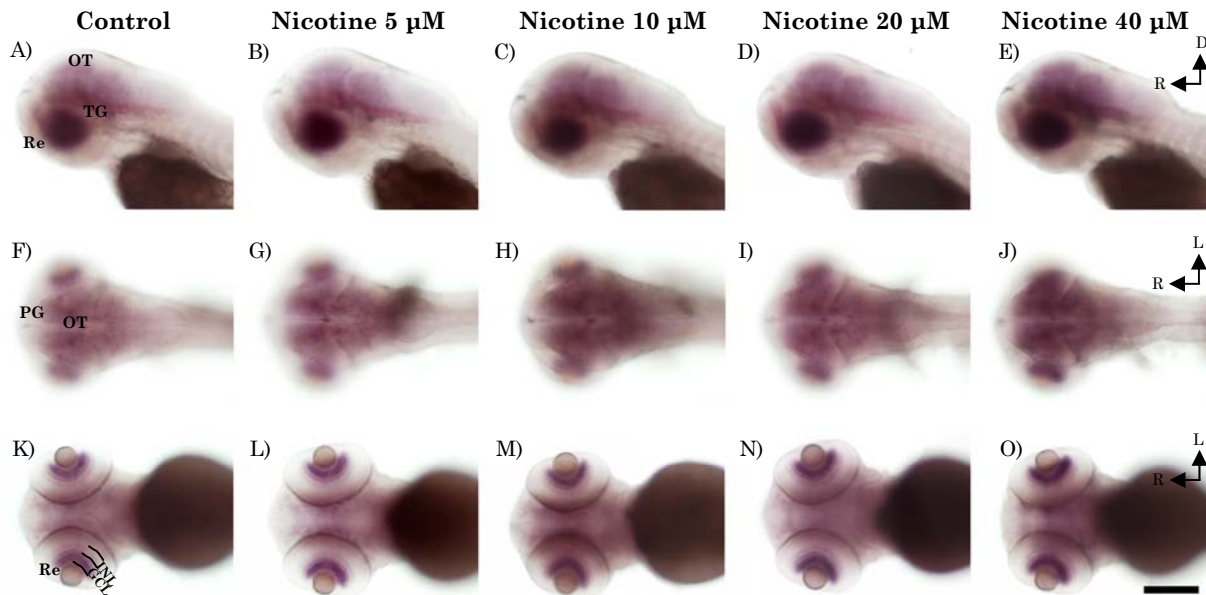
Fig. 11: *In toto in situ* **hybridization for α6 nAChR in 3 dpf larvae**. A)-E) Lateral view. F)-J) Dorsal view. K)-O) Ventral view. A), F) and K) Control animals are labeled in the OT. Expression is observed in the GCL of the retina and in isolated cells of the INL of the retina. Labeling is also observed in the pineal gland and trigeminal ganglion. The specimens treated with the higher concentrations of nicotine showed a greater intensity of staining in the visual and non-visual structures mentioned in the control group. D: Dorsal. GCL: Ganglion cell layer. INL: Inner nuclear layer. L: Lateral. OT: Optic tectum. PG: Pineal gland. R: Rostral. Re: Retina. TG: Trigeminal ganglion. Scale bar: 100 µm.

At the stage 48 hpf, ß3a nAChR is expressed in the GCL in the most central area of the retina . There was also labeling in the pineal gland in the trigeminal ganglion, and small groups of cells scattered throughout the brain. After hatching, at 3 dpf (Fig. 12) and 5 dpf, ß3a nAChR expression is maintained in the same structures as in the control group: GCL of the retina, pineal gland and trigeminal ganglion.

The ß3b nAChR analysis by qPCR technique provides expression values (Fig. 10C) showing, a decrease at the stage of 48 hpf, which is significant at the concentration of 5 µM. However, there is no significant increase in the expression of the receptor at 3 and 5 dpf.

Expression of ß3b nAChR was not detected by HIS technique at the stage of 48 hpf. Labeling appears after hatching, at 3 dpf (Fig. 13) and 5dpf. ß3b nAChR is expressed in the GCL of the central retina and in the trigeminal ganglion. At 5 dpf, the expression is observed in these same regions.

Fig. 12: *In toto in situ* **hybridization for β3a nAChR in 3 dpf larvae**. A)-E) Lateral view. F)-J) Dorsal view. K)-O) Ventral view. A), F) and K) Control animals present labeling in the GCL of the retina, and also in nonvisual structures as the pineal gland and the trigeminal ganglion. The animals treated with nicotine slightly increase the expression of this receptor in all treatment groups. This increase is observed in the same visual and non-visual structures mentioned in the control group. D: Dorsal. GCL: Ganglion cell layer. L: Lateral. OT: Optic tectum. PG: Pineal gland. R: Rostral. Re: Retina. TG: Trigeminal ganglion. Scale bar: 100 µm.
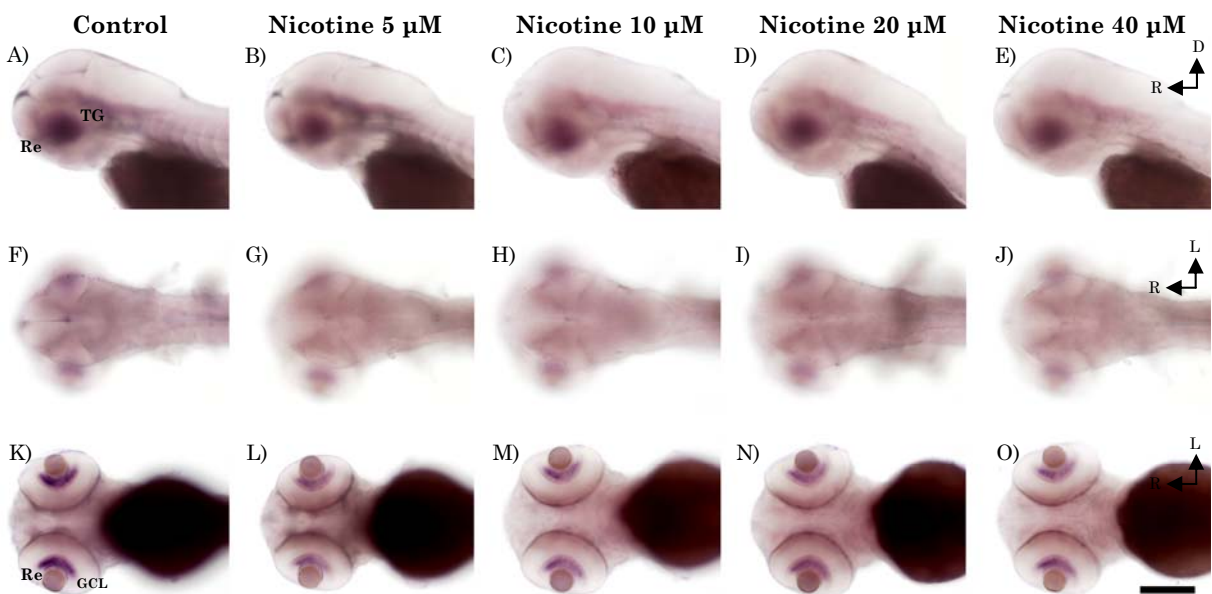
Fig. 13: *In toto in situ* **hybridization for β3b nAChR in 3 dpf larvae**. A)-E) Lateral view. F)-J) Dorsal view. K)-O) Ventral view. A), F) and K) Control animals present labeling in the retina, only in the central region of the GCL and in nonvisual structures as the trigeminal ganglion. At this stage, nicotine treated animals showed a decrease in the expression of this receptor in all treatment groups, being more pronounced in the group treated with 5 uM of nicotine. This decrease is observed in the same visual and non-visual structures mentioned in the control group. D: Dorsal. CCG: Ganglion cell layer. GT: Trigeminal ganglion. L: Lateral. R: Rostral. Re: Retina. Scale bar: 100 µm.

Electrophysiological analysis of the retina

The electroretinogram (ERG) records the summed electric field potential of the retina in response to light flashes and is a sensitive physiological tool to

Summary

assess radial retinal cell function (i.e., photoreceptor and bipolar cells). In zebrafish larvae, the ERG is dominated by a prominent b-wave which reflects mainly the responses of ON-bipolar cells (Wong *et al.*, 2004). The b-wave largely masks the response of the photoreceptors, the a-wave, which is not generally seen unless bright flashes are used. We elicited ERG responses over an intensity range of 5-6 log units. In control animals (Fig. 14), we observed a clear b-wave response at log I=-4, and with increasing flash intensities the b-wave grew larger reaching a peak amplitude with the brightest light tested (Log I=0).

In response to all concentrations of nicotine applied (Figs 14), two consistent changes in the ERG were noted. First, with a dim flash (Log I= -4), there was a decrease or loss of the b-wave. With brighter flashes (Log I= -2 and greater), the b-wave amplitude was increased, and at the highest doses (20 and 40 µM) of nicotine the increase was striking. Although b-wave amplitudes were
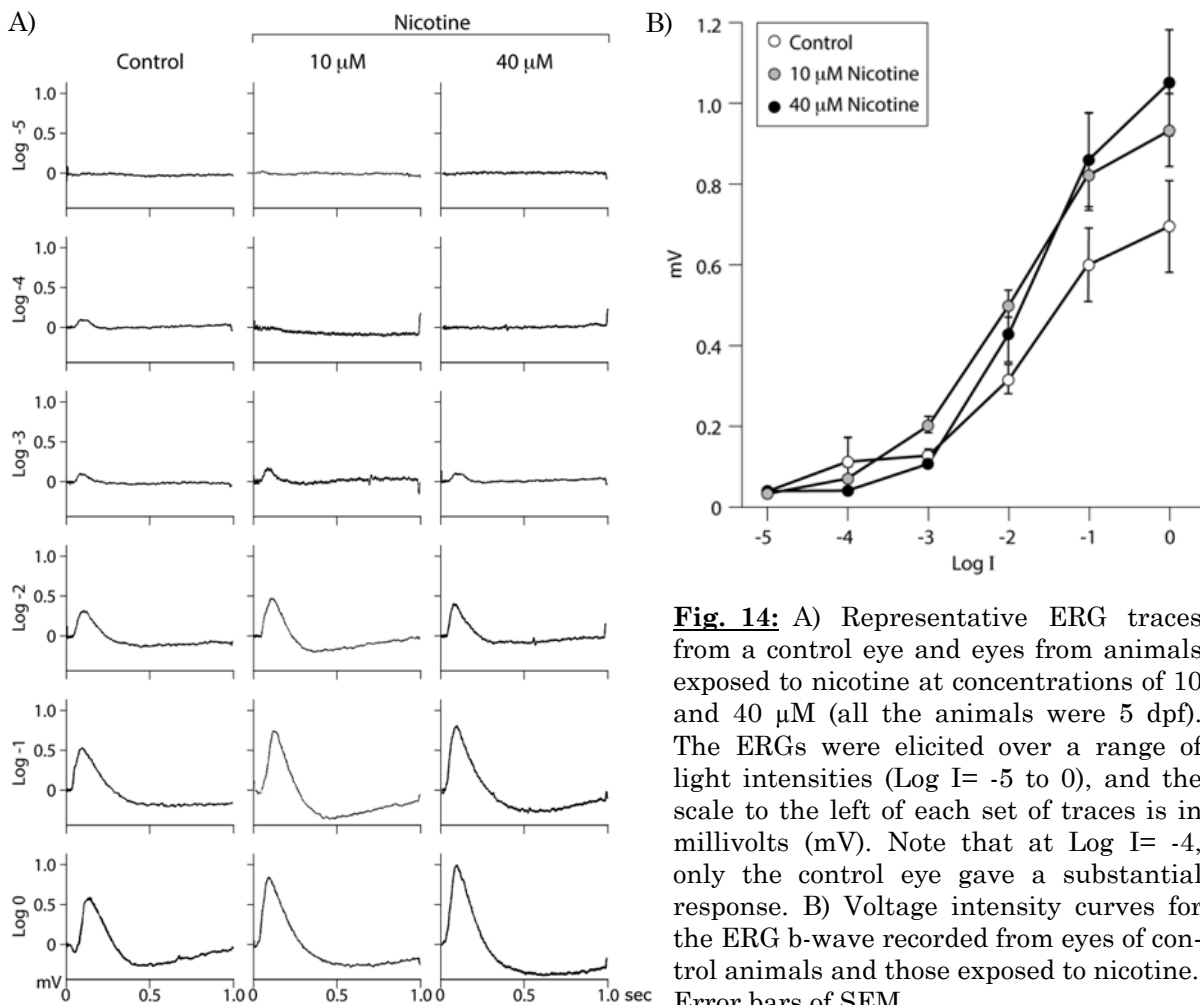
Fig. 14: A) Representative ERG traces from a control eye and eyes from animals exposed to nicotine at concentrations of 10 and 40 µM (all the animals were 5 dpf). The ERGs were elicited over a range of light intensities (Log I= -5 to 0), and the scale to the left of each set of traces is in millivolts (mV). Note that at Log I= -4, only the control eye gave a substantial response. B) Voltage intensity curves for the ERG b-wave recorded from eyes of control animals and those exposed to nicotine. Error bars of SEM.

enhanced at all light-intensities (except for the dimmest intensities), there was no significant change in the b-wave sensitivity to light.

The largest increase in amplitude was observed following the 20 µM dose of nicotine, and was an increase of 66%. At a concentration of 40 µM nicotine, the maximum amplitude decreased somewhat, suggesting that 20 µM nicotine may be the saturating concentration. However; the stimulus interval may have been too short (8 sec) at Log I=0 to allow complete recover from the previous flash.

The *nof* mutant has a point mutation the α subunit of the cone transducin (Tcα) gene, rendering it non-functional. All four types of cones in *nof* have undetectable levels of the Tcα protein. Not surprisingly, *nof* cones do not respond to photopic light stimulation (Brokerhoff *et al.*, 2003), but this enables recordings from the relatively few rods that exist at this point in zebrafish development. In nof mutants (Fig. 15), it is possible to record small b-wave responses over a range of 4 log units (Log I = -5 to -2). The maximum amplitude is about 40 µV, and that is observed at a light intensity of log I= -4. At light intensities brighter than Log I= -3, the b-wave response declines in amplitude and at log I= -1 or 0, no b-wave at all is recorded, probably due to rod saturation. With a nicotine concentration of 5 and 10 µM, a decrease in b-wave amplitude is observed at all light intensities, but because of the small rod response amplitudes in *nof* animals, the data are not significant (P=0.61 and 0.46 respectively). However, at a concentration of both 20 and 40 µM nicotine, the decrease in b-wave amplitude is significant (P=0.05 and 0.04 respectively).
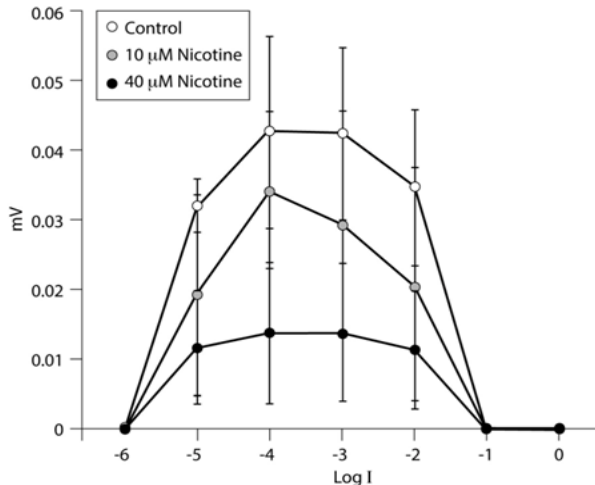
Fig. 15: ERG b-wave intensity curves recorded from the eyes of *nof* mutant fish that have no cone function. All animals were 5 dpf, and n=10. When fully dark-adapted small responses could be recorded at Log I = -5 to -2 (up to ~40 μM). At Log I = -1 and above, no responses could be elicited, presumably due to rod saturation. After nicotine treatment, all responses were smaller in amplitude. Error bars of SEM.

Behavioral analysis

Behavioral responses include visual-motor movements to escape, and simple swimming movements guided to catch food. A key visual response in zebrafish larvae is the optomotor response (OMR), in which there is a motor coordination to follow the movement. The optokinetic response (OKR) stabilizes the image on the retina during the free swimming. The visual-motor response (VMR) in zebrafish larvae is the startle response to changes in light intensity.

We have studied these different behavioral responses in larvae of 4, 5 and 6 dpf, to detect the neural alterations induced by nicotine in the visual context in relatively basic behaviors. In all responses, 4 dpf is the first stage in which this response appears, and we evaluated the answer later stage to assess the evolution of the response more time. We have analyzed various visual parameters such as contrast, spatial frequency and temporal frequency in control animals and in the groups treated with different concentrations of nicotine.

Optomotor response

Animals treated with different concentrations of nicotine have a significant decrease in the OMR (Fig. 16). Optomotor index decreases with

higher concentrations of nicotine. In animals treated with a nicotine concentration of 40 µM, the optomotor index is significantly reduced with respect to controls. Larvae treated with nicotine recovered activity levels with increasing contrast, but without reaching control levels.
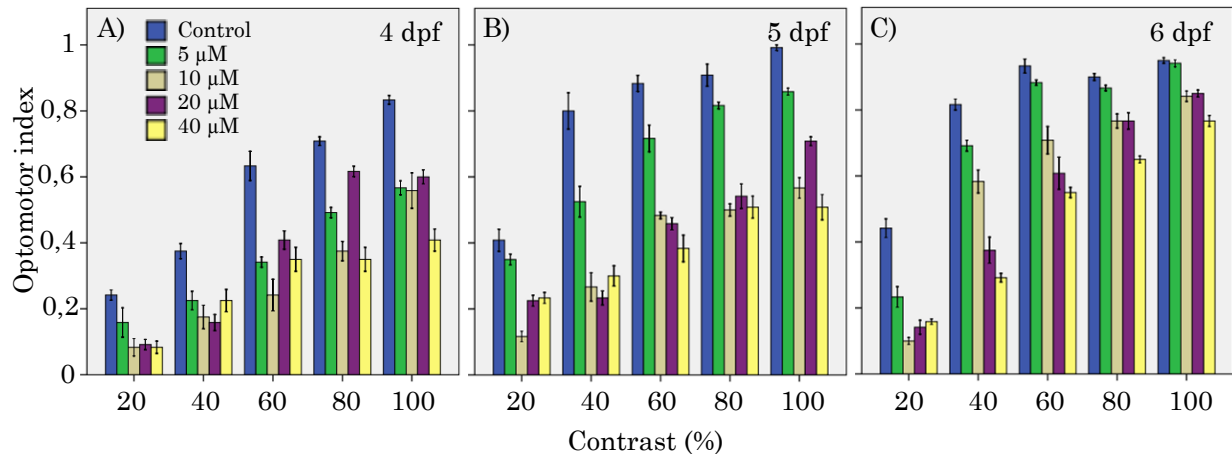

Fig 16: Behavioral measurements of contrast in the OMR at 4, 5 and 6 dpf. Average values of the optomor index, number of larvae that reach the end of the tank, by contrast values. Error bars indicate ± 1 standard error.

Optokinetic response

The animals treated with nicotine exhibit a speed difference in ocular movements with respect to the control group. This decrease varies depending on the concentration of nicotine administered (Fig. 17). Animals treated with 5 µM of nicotine showed the lower reduction. Other treatment groups show a less pronounced decrease. After increasing the contrast between black and white stripes, the decrease in eye movement speed persists. Animals treated with 40 µM of nicotine present the lowest speed of movement of the eyes.

Summary
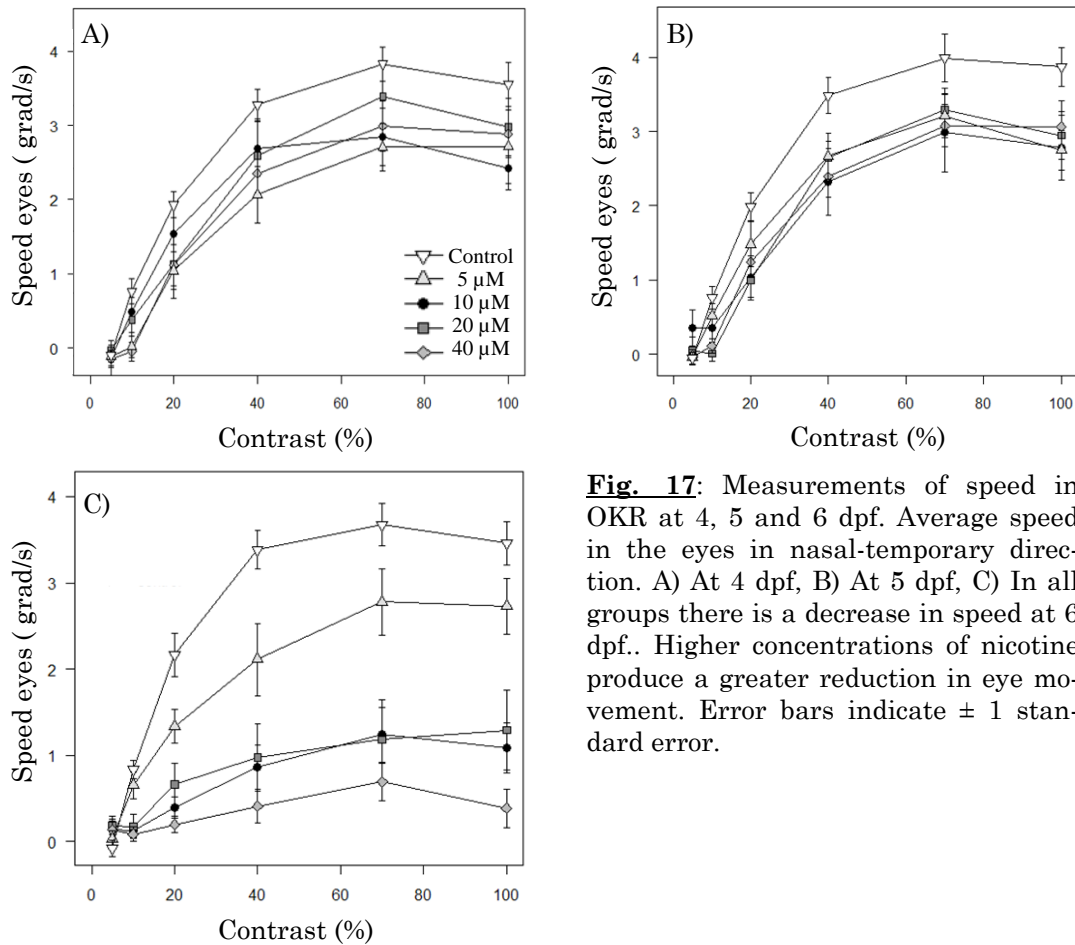
Fig. 17: Measurements of speed in OKR at 4, 5 and 6 dpf. Average speed in the eyes in nasal-temporary direction. A) At 4 dpf, B) At 5 dpf, C) In all groups there is a decrease in speed at 6 dpf.. Higher concentrations of nicotine produce a greater reduction in eye movement. Error bars indicate ± 1 standard error.

Visual-motor response

The VMR of control animals present the same activity and speed, with maximum when crossing from light to dark. At 5 dpf in treated animals (Fig. 18) swimming speed is lower than in the control group, and the reduction is greater in animals treated with 40 µM nicotine. The started swimming activity is higher than in controls. The activity and the speed of response to movement from light to dark is higher in those animals treated with a lower concentration of nicotine, while the activity and the change in the speed of movement from light to dark is lower in animals treated with higher doses of nicotine.
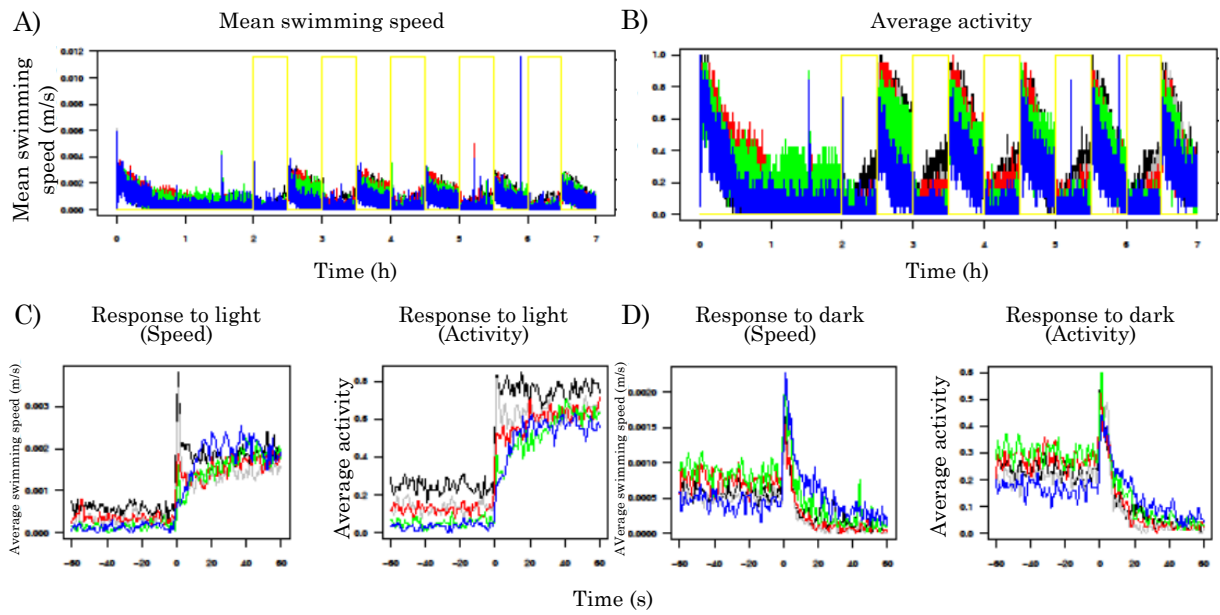
Fig. 75: Analysis of VMR at 5 dpf, showing the activity and average speed changes from light to dark and vice versa. A) Average swimming speed. B) Average activity of the larvae. C) Response of larvae to movement from dark to light. D) Response of larvae to movement from light to dark. In animals treated with nicotine both activity and swimming speed decrease. The greater decrease is observed in the group treated with 40 µM nicotine.

DISCUSSION

Effects of nicotine during zebrafish development

Early studies about the effects of nicotine date from the mid-nineteenth century (Haughton, 1872), whereas the use of zebrafish as a model to study the effects of nicotine on the development dates from the early XXI century (Sovoboda *et al.*, 2002). Nicotine produce different events processes during embryonic development, including gene expression, protein distribution, apoptosis, cellular proliferation and behavior (Svoboda *et al.*, 2002, Boyd *et al.*, 2003, Edwards, 2007; Parker and Connaughton, 2007 , Welsh *et al.*, 2009; Menelan and Svoboda, 2009; Thomas *et al.*, 2009).

Previous studies of chronic exposure to nicotine in zebrafish embryos indicate (Svoboda *et al.*, 2002, Parker and Connaughton, 2007; Menelaou and Svoboda, 2009; Thomas *et al.*, 2009, Welsh *et al.*, 2009). Our experimental design assure consistent levels of nicotine during the treatment. Analysis the different stages by HPLC demonstrated a constant assimilation of nicotine over time by the animals.

Effects of nicotine on the visual system

The zebrafish is a good model to study the development of the visual system and analyze how it is affected by exposure to different substances (Parng, 2005, Tierney, 2011). We have analyzed the effect of nicotine exposure on eye size, parameter that was estimated by measuring the projected area of the eye of the specimens in growth (Kashyap *et al.*, 2011). The measurements obtained were consistent, and the ocular area decreased significantly at the larval stages of 3 and 5 dpf in relation to the controls, especially in the treatments with nicotine concentrations, 20 and 40 μM.

Our results suggest that nicotine does not cause evident disturbances in the visual system at early stages of development. However, at later stages, when differentiation processes of the neural retina (36 hpf-3 dpf) occur, nicotine causes a delay in the pattern of cellular distribution. Previous studies in rats have shown a decrease in the thickness of the GCL and the INL of the retina (Evereklioglu *et al.*, 2003). Besides, chronic exposure to nicotine causes development delay in the lens and cataract formation (Evereklioglu *et al.*, 2004). It is considered that the loss of size in the structures may be due to a decrease in proliferation, increased cell death or a decrease in the number or volume of the of the cells. In our study, significant changes were not observed in the number of apoptotic cell process, in agreement with previous studies (Yan *et al.*, 2006). Markers associated with projections of the visual pathway, such as CR and Zn-8, showed that nicotine administration caused a decreased retinotectal projection to the OT that persists during the treatment.

We also observed a gradual decrease in the density of proliferative cells and a reduced extension of proliferative regions. This decrease is greater at higher concentrations of nicotine, which is in agreement with data obtained after administration of nicotine in neonatal rats, that causes inhibition of DNA synthesis, promoting premature termination of the proliferation and differentiation of cells (McFarland *et al.*, 1991).

Embryonic exposure to nicotine alters heterogeneously the expression of all molecular markers analyzed. The changes in cell types and/or regions of expression in the retina and the OT, vary with the dose of nicotine administered. Exposure to nicotine induces decrease in cell labeling CR positive cells in all visual areas, especially with higher concentrations of nicotine, but at the end of the larval period the distribution pattern of this calcium binding protein is similar to that observed in the control group. It has been suggested that during the development of the retina the expression of CR requires a minimum degree of tissue and cellular differentiation (Ellis *et al.*, 1991; Doldan *et al.*, 1999). The delay in CR immunostaining pattern observed in animals

treated with nicotine would be consistent with a delay in cellular differentiation of the neural retina.

The nicotine-treated specimens show a reduction in the distribution pattern of Zn-8 (a marker for Neuroline), in the retina, that can affect cell adhesion, growth and fasciculation of axons (Pourquie *et al.*, 1992), and synaptogenesis (Chedotal *et al.*, 1996). This might be interpreted as a neural plasticity response aimed to promote the growth and fasciculation of the first optic axons on their way towards the OT.

All brain regions involved in processing of visual information presented elements marked for TH. It has been studied in the zebrafish visual pathway the distribution pattern of TH in the retina (Guo *et al.*, 1999; Holzschuh *et al.*, 2001) and in diencephalic regions with retinal afferents (Rink and Wullimann, 2002; Wullimann and Rink, 2002). This may be due to an error in pretectal catecholaminergic cell migration, as the onset for TH immunoreactivity coincides in both regions (5 dpf) in control animals. In animals treated with nicotine, the density of TH positive cells decreases in all regions over time and the decrease is greater with higher doses of nicotine. These results are consistent with previous studies indicating that nicotine affects the expression of TH (Naha *et al.*, 2009). Furthermore, chronic administration of nicotine results in a decrease in the expression of the D2 dopamine receptor and TH protein transcriptional level, depending on the dose administered (Naha *et al.*, 2009).

Islet-1 is a specific marker of ganglion cells (Austin *et al.*, 1995) and its expression starts once they have completed their migration to the vitreal surface (Sakagami *et al.*, 2003). The alterations of the expression pattern of Islet-1 suggest that nicotine appears to affect more the later stages of retinogenesis (cellular differentiation of the visual structures) than early stages of retinal development (specification of neural and retinal pigment epithelium) (Schmitt and Dowling, 1994).

Pax6 is a transcription factor required for proper development of the optic vesicles (Zuber *et al.*, 2003), and its alteration can cause abnormalities in eye formation. Pax6 mutant mice exhibit a reduced size of the eyes and other encephalic structures (Theiler *et al.*, 1978, Hogan *et al.*, 1988, Glaser *et al.*, 1990, Fujiwara *et al.*, 1994, Hanson *et al.*, 1994, Dellovade *et al.*, 1998). Nicotine inhibits methylation of CpG noticeably, which is the binding site in the promoter StAR Pax6, which prevents binding of Pax6 and downregulates StAR gene expression (Wang *et al.*, 2011).

Effects of nicotine on nAChRs of the visual pathway

A series of studies relate very closely the α6 and ß3 nAChR subunits, showing a direct influence between them. Gotti *et al.* (2005) demonstrated that the ß3 nAChR gene suppression greatly reduces the α6 nAChR gene expression in different brain regions.

The tight regulation between these two subunits is also found in visual areas. At least seven subtypes of nAChRs are present in the rat retina (Moretti *et al.*, 2004; Marritt *et al.*, 2005) and many of these receptors are also found in the optic nerve. Sequential immunoprecipitation studies demonstrate that the optic nerve contains many of the nAChR α6 and ß3 subunits. In fact, the optic nerve has the largest number of α6 and ß3 nAChRs concentration found in the CNS (Cox *et al.*, 2008).

Chronic treatment with nicotine seems to alter the expression of the nAChRs (Marks *et al.*, 1992). In our study we have analyzed the expression levels by qPCR of α6, ß3a and ß3b subunits of nAChRs in zebrafish after administration of different doses of nicotine. The α6a nd ß3a subunits show similar values after treatment with nicotine in concentrations of 10, 20 and 40 µM. Acording to the temporal evolution, at 48 hpf there is a decrease in the expression while at 3 and 5 dpf there is an increase in expression. In addition,

the α6 subunit is expressed together with ß3a subunit in visual and non-visual anatomical regions both, that α6 and ß3b altogether do.

The α6 and ß3b subunits show similar expression values after treatment with a concentration of 20 μM nicotine of treatment. With respect to temporal evolution at 48 hpf the expression decreased more drastic in ß3b than α6, but at 3 dpf expression of ß3b continues to decrease in some treatments while than α6 to increase. At 5 dpf, both subunits, increases levels of expression. With respect to locating regions sharing α6 and ß3b limited to the visual structures in CCG of the retina and non-visual, such as trigeminal ganglion.

The expression of α6 nAChR in the visual system and the mammalian retina suggests that this subunit is important in vision (Moretti *et al.*, 2004, Millar and Gotti, 2009). In mice, after injection of nicotine the expression of the nAChR α6 subunit increases dopaminergic neurons of the ventral tegmental area, concluding that high doses of nicotine selectively activates dopaminergic neurons (Zhao-Shea *et al.*, 2011).

Zebrafish has a duplicate gene for nAchR ß3 subunit, the nAChR ß3a and nAchR ß3b. Our study shows that nicotine produces different effects in each of these receptors. Mattes *et al.* (1995) indicate that expression of ß3 nAChR affects the fate of ganglion cells in the developing retina.

Effects of nicotine in electrophysiology of the retina

Our results show that nicotine enhances greatly cone-driven b-wave amplitudes in larval zebrafish, but significantly depresses rod-driven b-wave amplitudes. These results clarify and extend the earlier results in rabbits (Jurklies *et al.*, 1996) and humans (Varghese *et al.*, 2011) that suggested nicotine may enhance the b-wave under photopic conditions and decrease the b-wave under scotopic conditions. Whereas nicotine greatly altered both cone and rod driven b-wave amplitudes, it did not affect the sensitivity of the responses.

It is unclear how nicotine might affect b-wave amplitudes. Assuming that the b-wave in zebrafish directly reflects ON-bipolar cell responses, our data suggest that nicotine increases the light response in cone ON-bipolar cells, but decreases the light response in rod ON-bipolar cells, but how this is mediated is unclear. Bipolar cell light responses are believed to be generated in the outer plexiform layer (OPL), as a result of synaptic input onto the bipolar cells from the photoreceptors. In larval zebrafish, Arenzana *et al.*, (2005) have observed processes containing choline acetyltransferase (ChAT) in the OPL, and it may be that these processes are the source of the acetylcholine that affects the bipolar cells. The processes containing ChAT gradually disappear as the larvae mature, and in the adult zebrafish processes containing ChAT are found only in the IPL.

In zebrafish, however, whereas there are bipolar cells that receive input only from cones, all of the bipolar cells that receive rod input also have cone input (Li *et al.*, 2012). However, of the four mixed rod-cone bipolar cells in zebrafish, one has the great majority (6 times) of its input from rods; the others have more input from cones than rods. Also, all of the rod-dominated bipolar cells are ON-cells, whereas most of the bipolar cells receiving mixed rod-cone input are OFF-cells or ON-OFF cells. It may be that the rod dominant mixed bipolar cell is the main contributor to the scotopic b-wave in zebrafish, and it is this cell whose activity is strongly depressed by nicotine, whereas the other ON-bipolar cells give a mixed or no response to nicotine. In *nof* mutants the mixed rod-cone bipolar cells receive no cone input, perhaps enhancing the rod suppression of the b-wave.

Interestingly, whereas an a-wave is usually readily observed with bright stimuli in control fish. We interpret our data to mean that nicotine substantially enhances cone b-wave activity and quickens it, but may depress rod b-wave responses. However, as noted earlier, zebrafish larvae are highly cone dominant, and rod responses are difficult to isolate because of the very large cone responses. Therefore, we turned to a mutant (*nof*) fish that has no cone function to better evaluate the effects of nicotine on the rod-driven b-wave.

Effects of nicotine in the behaviour induced by visual function

The optomotor response (OMR) test evaluates the effect of compounds on zebrafish vision with higher performance optokinetic response (OKR). However, compounds that affect the locomotive capacity of zebrafish could generate positive response in the OMR test. Therefore, the OMR test can be used as a screen for compounds which cause defects in the visual function and a secondary screening with OKR and hypomotility in a locomotor test (Richards *et al.*, 2008).

The results we observed in optomotor response analysis indicate a deficit in tracking visual stimulus, which may be influenced by hypomotility problems in nicotine treated animals (Svoboda *et al.*, 2002). Certain component of the change in the response is due to a vision problem, since the increasing in contrast, spatial frequency or temporal frequency, improves OMR.

The use of eye movement measurements has been very useful for understanding neurophysiological and neurochemical dysfunction after administration of different drugs or clinical conditions (Maurer *et al.*, 2011). Behavioral studies in animal models and humans exposed to different drugs indicate that oculomotor measures can provide a highly sensitive index of pharmacodynamic drug effect on brain systems (Reilly *et al.*, 2008). OKR is altered after administration of nicotine. With a speed diminution in eye tracking associated to a visual stimulus. Furthermore, saccades decrease in nicotine treated animals, which is consistent with data from humans (Clarke *et al.* 1985; Domino *et al.*, 1997; Larrison *et al.*, 2004; Rycroft *et al.*; 2006 Zingler *et al.*, 2007). These studies have shown that nicotine reduces the number of primary saccades during search tasks in smokers, non-smokers and in patients with schizophrenia (Avila *et al.,* 2003; Olincy *et al.*, 2003, Tanabe *et al.* 2006).

Circadian factors, such as the light-dark cycle, have effects on the development of the visual system (Hainline and Abramov, 1991; Organisciak and Winkler, 1994; Guido *et al.*, 2010). Thus, adverse lighting conditions affect

the retinal anatomy. In this sense, studies suggest that alterations in ilumination can produce substantial damage (Hainline and Abramov, 1991), while other studies indicate that this cirscunstance, even during long periods of time (up to 8 months) have little effects on the retinal anatomy (Bilotta, 2000). In our results of VMR show that zebrafish treated with low doses of nicotine respond similarly to the light stimulus than control animals, whereas the increase in the dose of nicotine decreases the response to light stimulation. This indicates the possible development of a deficit in visual accommodation with respect to the movement from light to dark. In studies with rats in which visual stimuli have been employed on and off of the light in dwellings, it has been found that nicotine increases the sustained response rates for both stimulus changes (Raiff and Dallery, 2009), althought the association of the stimulus with food may have interfered with the results.

CONCLUSIONS

According to the objectives of this Doctoral Thesis, and as a consequence of the results and discussion, we have concluded that:

I. Exposure of zebrafish embryos to nicotine reduces the ocular area and the size of the animal in relation to the dose administered, without affecting the lamination of either the retina or the optic tectum.

II. Exposure of zebrafish embryos to nicotine causes less pronounced effects during the segregation between the neural retina and the retinal pigment epithelium, than during cell differentiation of the neural retina, which is associated with a delay in the neurochemical maturation of different populations of the neural retina.

III. The treatment with nicotine during development alters the expression patterns of nAChRs. ß3a and α6 subunits increase after treatment with increasing doses of nicotine. ß3b and α6 subunits differ in their expression levels in different nicotine treatment groups and at different stages of development analyzed.

IV. Nicotine alters the electroretinogram in zebrafish, stimulating ON bipolar cells that receive cone input and inhibiting ON bipolar cells with rod input.

V. Animals exposed to low concentrations of nicotine present a correct motor activity but an impairment in visual skills, whereas animals exposed to higher concentrations of nicotine have increased visual deficits and problems in motor activity appear.